

Sources and trends of trace elements and
polycyclic aromatic hydrocarbons in a
shallow lake in the Mediterranean area from
sediment archives of the Anthropocene

Paola Gravina^{1*}, Bartolomeo Sebastiani¹, Federica
Bruschi¹, Chiara Petroselli¹, Beatrice Moroni¹, Roberta
Selvaggi¹, Enzo Goretti¹, Matteo Pallottini¹, Alessandro
Ludovisi¹ and David Cappelletti¹

^{1*}Department of Chemistry Biology and Biotechnology, University
of Perugia, via Elce di Sotto 8, Perugia, 60123, Umbria, Italy.

*Corresponding author(s). E-mail(s): paolagravi@gmail.com;
Contributing authors: bartolomeo.sebastiani@unipg.it;
federica.bruschi@studenti.unipg.it; petrosellichiaara@gmail.com;
b.moroni@tiscali.it; roberta.selvaggi@unipg.it;
enzo.goretti@unipg.it; matteo.pallottini@unipg.it;
alessandro.ludovisi@unipg.it; david.cappelletti@unipg.it;

SUPPLEMENTARY MATERIAL

1 Chemical analysis

1.1 Major and trace elements

Major and trace elements (Al, Fe, Ti, V, Mn, Co, Ni, Pb, Cr, Cu, Zn and P, and corresponding wavelengths in Table SM1) concentrations were determined by Inductively Coupled Plasma an Optical Emission Spectrometry (ICP-OES, Ultima 2, HORIBA Scientific) equipped with an ultrasonic nebulizer (CETAC Technologies, U-5000AT). The sediment samples were first dried at 105 °C for 24 h, then an aliquot (0.250 g) was digested with 8 ml of ultrapure HNO₃ (65-69%) and 2 ml of ultrapure H₂O₂ (30-32%). The acid digestion was performed in a Mars Microwave Oven, with 2 working steps: the first at 130 °C (200 psi) for 1' and the second at 180 °C (300 psi) for 10'. The digestion mixture was finally filtered using 2,5 μm filters (Whatman Grade n 42), and diluted to 50 ml with ultrapure H₂O (18 MΩ). Quality assurance was provided by determining the elemental concentrations for duplicate samples and one reference material (Certified Reference material SS-1-Contaminated Soil). The recovery of total metal concentration varied between 79 and 130% among the different analytes. The Limit of Detection (LOD) of the methods ranged from 0.01 to 2.95 ppm (Table SM2).

1.2 Organic compounds

An amount between about 2 to 4g dry weight of powdered sediment was spiked before extraction with a mix of 13 perdeuterated surrogate homologues as recovery standards (namely naphthalene-d₈, acenaphthene-d₈, phenanthrene-d₁₀, fluoranthene-d₁₀, pyrene-d₁₀, chrysene-d₁₂, benzo(b)fluoranthene-d₁₂, Benzo(a)pyrene-d₁₂, perylene-d₁₂, debenzo(a,h)anthracene-d₁₂, benzo(ghi)perylene-d₁₂ and dibenzo(a,i)pyrene-d₁₄, to monitor recovery method (average recovery >70%). The PAH fractions

28 were extracted twice in dichloromethane (DCM) by ultrasonic agitation at
29 ambient temperature for 15min. Then, the combined extracts were fraction-
30 ated by adsorption chromatography on activated silica gel (high-purity grade,
31 pore size 60 , 70-230 mesh ASTM, Merck, Germany), pre-conditioned overnight
32 at 120°C. The PAHs were isolated by elution with 20ml of a n-hexane-
33 dichloromethane solution (4:1 ; v/v) and reduced to small volume. The residues
34 was resuspended in 80 μ l for GC-MS analysis. An aliquot of 0.5 μ l in n-hexane
35 was analysed using a gas chromatography-mass spectrometry with a triple-axis
36 detector (HP7890A/5975CVL - Agilent Technologies, USA), equipped with
37 low bleed Select-PAH capillary column (Agilent J&W, CP 7461), 15mx0,15mm
38 ID and 0,10 μ m film thickness.+ 3m EZ-Guard.

39 GC oven programmed conditions were: from 80° (kept 0.8 min.) to 180°C at
40 70°C/min., to 230°C at 7°C/min. (kept 7 min.), to 280°C at 50°C/min. (kept 7
41 min.) and to 350°C at 30°C/min. (kept 7 min.) High purity Helium was used as
42 carrier gas at constant flow rate of 1.2 ml/min and the injector operated under
43 pulsed splitless mode (50psi for 0.4 min.) at 300°C. The mass detection was
44 performed in selected ion monitoring (SIM) mode with ion source operating in
45 electron positive ionisation at a voltage of 70eV and temperature of 230°C. All
46 the reagents used for the analytical procedure, extraction and clean-up were
47 analytical grade of highest purity or high performance liquid chromatography
48 (HPLC) grade (\geq 99%) and purchased from the Sigma-Aldrich, Deisenhofen,
49 Germany. The analytical standard of PAHs and their perdeuterated surrogate
50 homologues were supplied by BCR Certified Reference Material CEE, Lab Ser-
51 vice Analytica-Dr. Ehrenstorfer GmbH (Italy-Germany) and Neochema GmbH
52 (Germany). The procedure was defined according to ISTISAN 99/28 (Italian

53 National Health Service, 1999), an extensively consolidated method for qual-
54 ity assurance and quality control (QA/QC) in analysis of Persistent Organic
55 Pollutants (POPs) in sediments.

56 **1.3 Lead isotope analysis**

57 The determination of $^{208}\text{Pb}/^{207}\text{Pb}$ and $^{206}\text{Pb}/^{207}\text{Pb}$ ratios was performed by
58 an Agilent 8900 ICP-MS/MS (100 version, Agilent Technologies, Japan), oper-
59 ated in the MS/MS mode. The instrument is equipped with two quadrupole
60 mass units (Q1 and Q2) and a third generation octopole-based collision/re-
61 action cell system (CRS) located in-between (Q1-CRC-Q2). A micro mist
62 nebulizer and a spray chamber kept at 4°C were used for the sample intro-
63 duction. The CRC was pressurized with a NH_3/He 15 % mixture, used as a
64 damping gas to lower the RSD. Q1 and Q2 were both set on mass $m/z =$
65 206, 207 and 208. The integration time for each isotope mass was set to 1 sec-
66 ond with 4000 sweeps. Internal precision was 0.56% (%RSD, $n = 10$) for the
67 $^{206}\text{Pb}/^{207}\text{Pb}$ ratio. The instrumental mass bias was corrected with the stan-
68 dard sample bracketing method using the lead isotopic standard SRM 981
69 from NIST (Gaithersburg, MD, USA) [Vanhaecke et al \(2009\)](#). More details on
70 the method are reported in [Bazzano and Grotti \(2014\)](#); [Bazzano et al \(2021\)](#);
71 [Bertinetti et al \(2022\)](#)).

72 **Acknowledgments.** We thank MIUR and University of Perugia for finan-
73 cial support through AMIS project (“Dipartimenti di Eccellenza–2018–2022”).

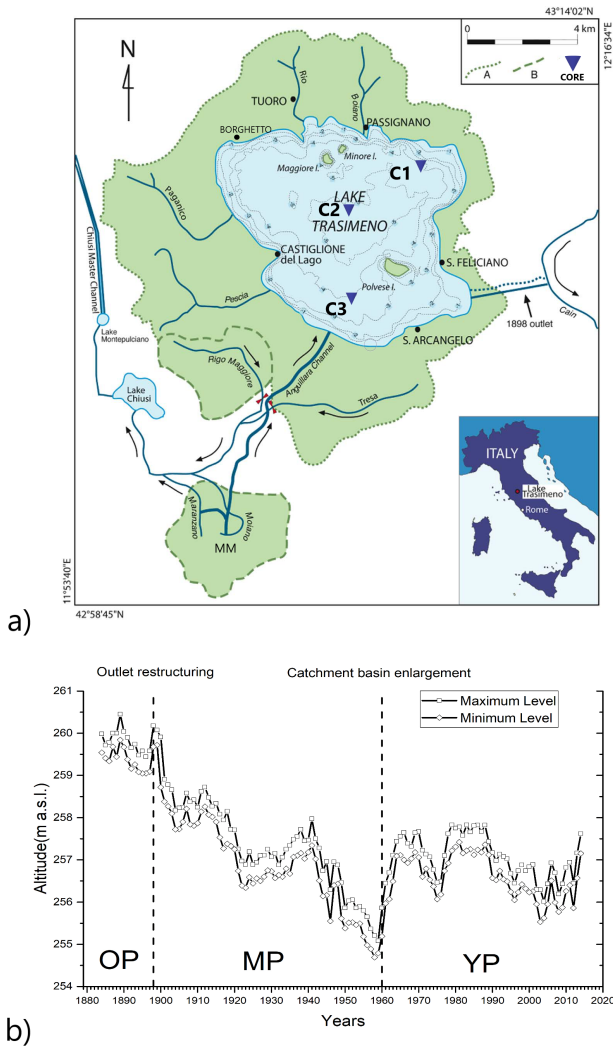


Fig. SM1: *a*) map of the Trasimeno lake with its catchment basin (modified from [Marchegiano et al \(2018\)](#)), A) natural catchment area, B) artificially-joined basins of Rigo Maggiore (RM) and Moiano and Maranzano (MM, is joined to the lake by artificial canal crossing over the natural waterway). The blue triangles mark the location of sampling sites (C1,C2 and C3 cores located at the coordinates N 43°09'40.0" E 12°10'06.0", N 43°08'38" E 12°06'43" and N 43°05'51" E 12°06'38", respectively). *b* shows the trend of water level, with hydrometric phases, old (OP), middle (MP) and young (YP) are indicated.

Sample	Depth	Dating	Sample	Depth	Dating	Sample	Depth	Dating
code	cm	years	code	cm	years	code	cm	years
C2-1	1	2007	C1-1e2	1 e 2	2006	C3-1e2	1 e 2	2003
C2-2	2	2005	C1-3	3	2003	C3-3	3	2000
C2-3	3	2004	C1-4	4	2001	C3-4	4	1997
C2-4	4	2003	C1-5	5	1999	C3-5	5	1994
C2-5	5	2001	C1-6	6	1997	C3-6	6	1991
C2-6	6	2000	C1-7	7	1996	C3-7	7	1988
C2-7	7	1999	C1-8	8	1994	C3-8	8	1985
C2-8	8	1997	C1-9	9	1992	C3-9	9	1982
C2-9	9	1996	C1-10	10	1990	C3-10	10	1979
C2-10	10	1994	C1-11	11	1989	C3-11	11	1976
C2-11	11	1993	C1-12	12	1987	C3-12	12	1973
C2-12	12	1992	C1-13	13	1985	C3-13	13	1970
C2-13	13	1990	C1-14	14	1984	C3-14	14	1967
C2-14	14	1989	C1-15	15	1982	C3-15	15	1964
C2-15	15	1988	C1-16	16	1980	C3-16	16	1961
C2-16	16	1986	C1-17	17	1978	C3-17	17	1958
C2-17	17	1985	C1-18	18	1977	C3-18	18	1955
C2-18	18	1984	C1-19	19	1975	C3-19	19	1952
C2-19	19	1982	C1-20	20	1973	C3-20	20	1949
C2-20	20	1981	C1-21	21	1972	C3-21	21	1946
C2-21	21	1979	C1-22	22	1970	C3-22	22	1943
C2-22	22	1978	C1-23	23	1968	C3-23	23	1940
C2-23	23	1977	C1-24	24	1966	C3-24	24	1937
C2-24	24	1975	C1-25	25	1964	C3-25	25	1934
C2-25	25	1974	C1-26	26	1962	C3-26	26	1931
C2-26	26	1973	C1-27	27	1960	C3-27	27	1928
C2-27	27	1971	C1-28	28	1957	C3-28	28	1925
C2-28	28	1970	C1-29	29	1956	C3-29	29	1922
C2-29	29	1968	C1-30	30	1955	C3-30	30	1919
C2-30	30	1967	C1-32	32	1951	C3-32	32	1915
C2-32	32	1965	C1-34	34	1948	C3-34	34	1909
C2-34	34	1962	C1-36	36	1944	C3-36	36	1903
C2-36	36	1960	C1-38	38	1941	C3-38	38	1897
C2-38	38	1957	C1-40	40	1937	C3-40	40	1891
C2-40	40	1954	C1-42	42	1934	C3-42	42	1885
C2-42	42	1951	C1-44	44	1930	C3-44	44	1879
C2-44	44	1949	C1-46	46	1927	C3-46	46	1873
C2-46	46	1946	C1-48	48	1924	C3-48	48	1867
C2-48	48	1943	C1-50	50	1921	C3-50	50	1861
C2-50	50	1940	C1-52	52	1918			
C2-52	52	1938	C1-54	54	1915			
C2-54	54	1935	C1-56	56	1912			
C2-56	56	1932	C1-58	58	1909			
C2-58	58	1929	C1-60	60	1906			
C2-60	60	1927	C1-62	62	1903			
C2-62	62	1924	C1-64	64	1900			
C2-66	66	1918	C1-66	66	1897			
C2-68	68	1916	C1-68	68	1895			
C2-70	70	1913	C1-70	70	1892			
C2-72	72	1910	C1-72	72	1889			
C2-74	74	1908	C1-74	74	1887			
C2-76	76	1905	C1-76	76	1884			
C2-78	78	1902	C1-78	78	1881			
C2-80	80	1899	C1-80	80	1879			
C2-82	82	1897	C1-82	82	1876			
C2-84	84	1894	C1-84	84	1874			
C2-86	86	1891	C1-86	86	1871			
C2-88	88	1888	C1-88	88	1868			
C2-90	90	1886	C1-90	90	1865			
C2-92	92	1883	C1-92	92	1863			
C2-94	94	1880	C1-95	95	1859			
C2-96	96	1877						
C2-98	98	1875						
C2-100	100	1872						
C2-102	102	1869						

Fig. SM2: The table shows the sub-sample lists for all 3 sediment cores. Each sample is associated with: an alphanumeric code, depth to surface and corresponding date.

Table SM1: Measurement wavelengths by ICP-OES.

Element	λ (nm)
Zn	213,856
P	214,914
Ni	216,556
Pb	220,353
Co	228,616
Al	237,312
Mn	257,61
Fe	259,94
V	292,402
Cr	267,716
Ti	323,452
Cu	327,396

Table SM2: LOD values per element are reported.

Element	LOD		
	C1	C2	C3
Mg	2,69	1,07	2,69
Fe	0,12	0,22	0,12
Al	1,01	0,12	1,01
Ca	2,95	0,56	2,95
K	2,63	0,32	2,63
V	0,09	0,02	0,26
Co	0,12	0,02	0,20
Ni	0,09	0,03	0,10
Pb	0,07	0,02	0,19
Cr	0,06	0,01	0,20
Cu	0,04	0,01	0,37
Ti	0,01	0,04	0,28
Zn	0,03	0,03	0,08
P	0,03	0,03	0,15
Mn	0,01	0,16	0,05

75 References

- 76 Bazzano A, Grotti M (2014) Determination of lead isotope ratios in envi-
77 ronmental matrices by quadrupole ICP-MS working at low sample
78 consumption rates. *Journal of Analytical Atomic Spectrometry* 29(5):926.
79 doi:<https://doi.org/10.1039/c3ja50388g>
- 80 Bazzano A, Bertinetti S, Ardini F, et al (2021) Potential Source Areas for
81 Atmospheric Lead Reaching Ny-Ålesund from 2010 to 2018. *Atmosphere*

8 REFERENCES

	Element	Mean Bottom below 76 cm	dev sta	Mean upper 76 cm	dev sta	Mean whole core	dev sta
C1	Co	10,7	3,7	13,1	2,2	12,7	2,6
	Ni	109,0	10,9	99,1	12,8	100,7	13,0
	P	1497,8	77,3	1723,6	304,7	1686,6	292,2
	Pb	13,5	2,6	18,6	2,8	17,8	3,3
	Cr	144,1	10,2	131,3	13,7	133,4	14,0
	Cu	24,4	8,4	32,3	5,7	31,0	6,8
	Ti	406,8	65,2	317,4	70,3	332,0	76,6
	Zn	87,2	19,4	97,8	28,6	96,0	27,5
	Mn	781,0	64,4	829,6	105,5	821,7	101,1
	V	73,2	8,6	77,0	11,5	76,4	11,1
C2	Co	20,5	1,5	19,6	4,4	19,8	4,0
	Ni	117,4	6,7	101,3	25,1	104,8	23,3
	P	2310,9	119,9	2448,7	223,8	2419,0	212,8
	Pb	19,6	1,3	22,6	2,8	22,0	2,8
	Cr	183,4	17,2	158,8	39,8	164,1	37,5
	Cu	25,2	1,9	24,2	2,7	24,4	2,6
	Ti	514,4	118,0	446,9	121,2	461,8	122,8
	Zn	115,2	8,5	111,9	21,6	112,6	19,5
	Mn	815,7	117,6	1312,5	388,9	1205,5	404,1
	V	98,3	11,6	93,2	15,8	94,3	15,1
C3	Co	4,9	3,5	8,8	4,0	7,9	4,2
	Ni	71,9	6,6	80,8	11,0	78,6	10,7
	P	1277,8	183,8	1323,3	155,6	1311,2	161,9
	Pb	9,4	1,9	14,2	2,3	13,0	3,0
	Cr	90,8	13,9	111,6	19,7	106,4	20,4
	Cu	13,0	2,0	19,6	3,0	18,0	4,0
	Ti	307,2	63,7	356,2	121,8	343,3	110,7
	Zn	58,6	9,2	86,9	37,3	79,8	34,8
	Mn	709,6	58,4	730,8	111,0	725,5	100,1
	V	47,1	7,9	69,7	13,4	64,1	15,7
Current State	Co	7,7	3,7				
	Ni	76,6	16,2				
	P	418,6	79,1				
	Pb	18,8	3,0				
	Cr	100,0	27,6				
	Cu	18,2	4,1				
	Ti	292,5	104,4				
	Zn	78,5	13,1				
	Mn	1063,9	303,9				
	V	53,3	17,6				

Table SM3: Average, maximum and minimum concentrations (unit mg/Kg) for the whole sediment cores (C1,C2,C3), average of the anthropized (upper) and average of the pristine (bottom) section are reported.

- 82 12(3):388. doi:<https://doi.org/10.3390/atmos12030388>
- 83 Bertinetti S, Bolea-Fernandez E, Malandrino M, et al (2022) Strontium iso-
- 84 topic analysis of environmental microsamples by inductively coupled
- 85 plasma – tandem mass spectrometry. Journal of Analytical Atomic
- 86 Spectrometry 37(1):103–113. doi:<https://doi.org/10.1039/D1JA00329A>

Table SM4: Principal component analysis on C2 core, by euclidean distance and complete method. The principal component values major are highlighted in each column.

Element	Component		
	PC1	PC2	PC3
Mn	-0.276	0.203	0.351
Fe	0.192	0.106	0.498
Al	0.246	-0.366	0.384
V	0.357	-0.164	0.150
Co	0.356	0.238	-0.032
Ni	0.351	0.200	-0.166
Pb	0.153	0.503	0.310
Cr	0.378	0.018	-0.030
Cu	0.014	-0.405	-0.075
Ti	0.248	-0.419	0.191
Zn	0.355	0.194	-0.011
P	-0.168	-0.175	0.435
PAHs	-0.256	0.169	0.318
Proportion of Variance	0.522	0.146	0.128
Cumulative Proportion	0.522	0.667	0.796

- 87 Marchegiano M, Francke A, Gliozzi E, et al (2018) Arid and humid phases
88 in central Italy during the Late Pleistocene revealed by the Lake Trasi-
89 meno ostracod record. *Palaeogeography, Palaeoclimatology, Palaeoecol-*
90 *ogy* 490:55–69. doi:<https://doi.org/10.1016/j.palaeo.2017.09.033>
- 91 Vanhaecke F, Balcaen L, Malinovsky D (2009) Use of single-collector and
92 multi-collector ICP-mass spectrometry for isotopic analysis. *Journal of*
93 *Analytical Atomic Spectrometry* 24(7):863. doi:[https://doi.org/10.1039/](https://doi.org/10.1039/b903887f)
94 [b903887f](https://doi.org/10.1039/b903887f)

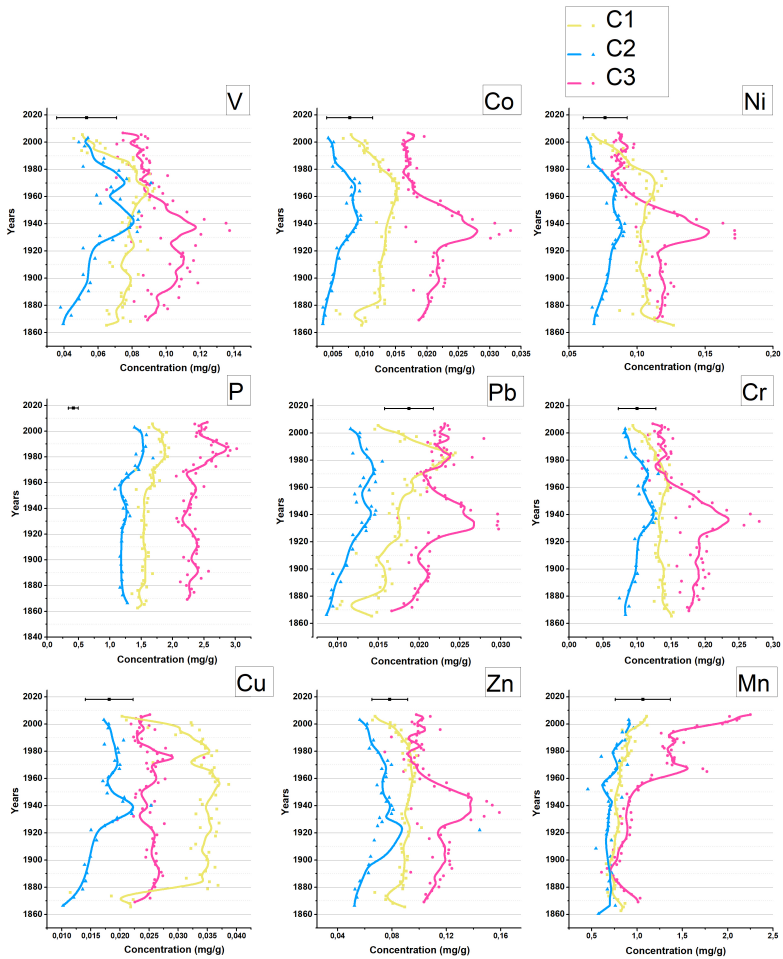


Fig. SM3: Trace element concentration trends (V, Co, Ni, P, Pb, Cr, Cu, Zn and Mn) in the three sediment cores: C1 (yellow), C2 (pink), C3 (blue) (adjacent-averaging method, with weighted average options was used on 5 points to obtain the trends line). The scatter represent single samples analysed and the line represents moving averages every 5 years. The black square represents the current concentration in the surface sediments (corresponding to 2018) and the error bar represents standard deviation.

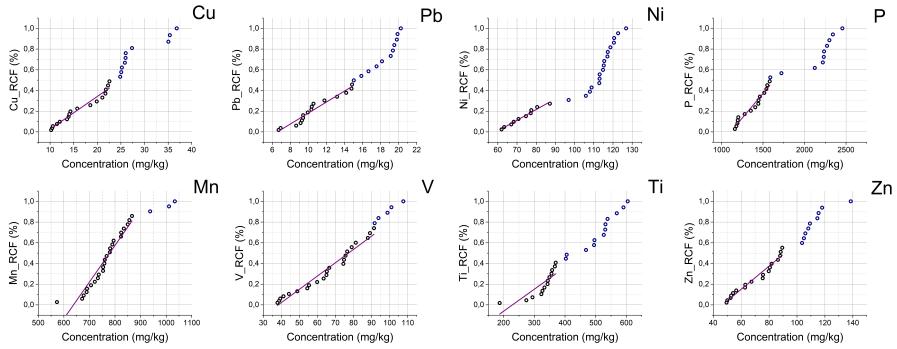


Fig. SM4: Cumulative frequency curves (scatters) of Cu, Pb, Ni, P, Mn, V, Ti and Zn. Linear regressions were performed on the cumulative frequency curve with $p < 0.01$ and $R^2 > 0.9$ (purple line).

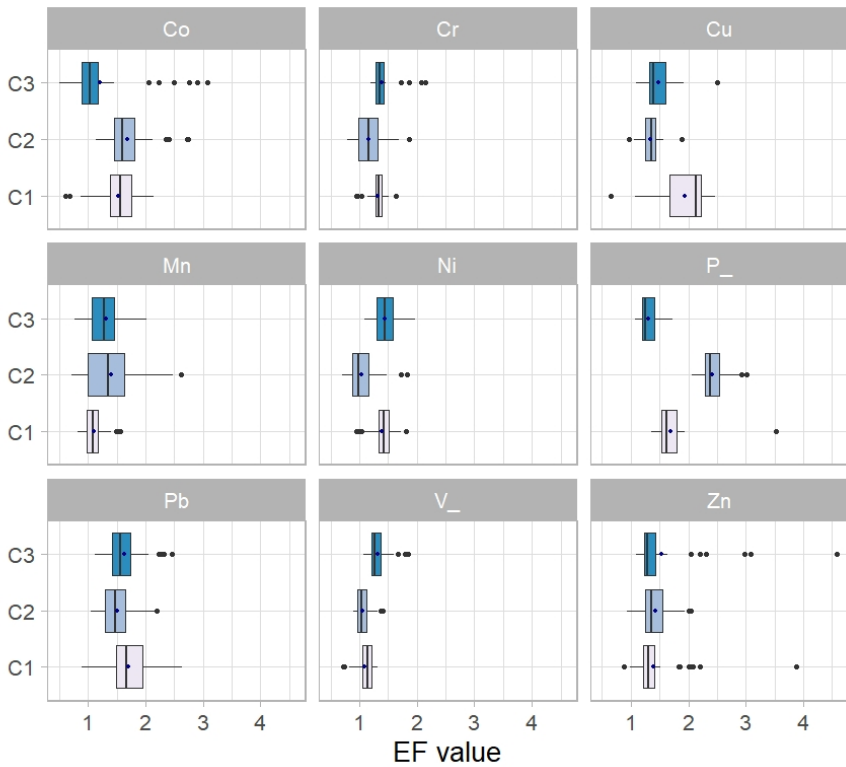


Fig. SM5: Boxplot of Enrichment factor for trace elements calculated for the 3 sediment cores. The mean values are represented by blue point.

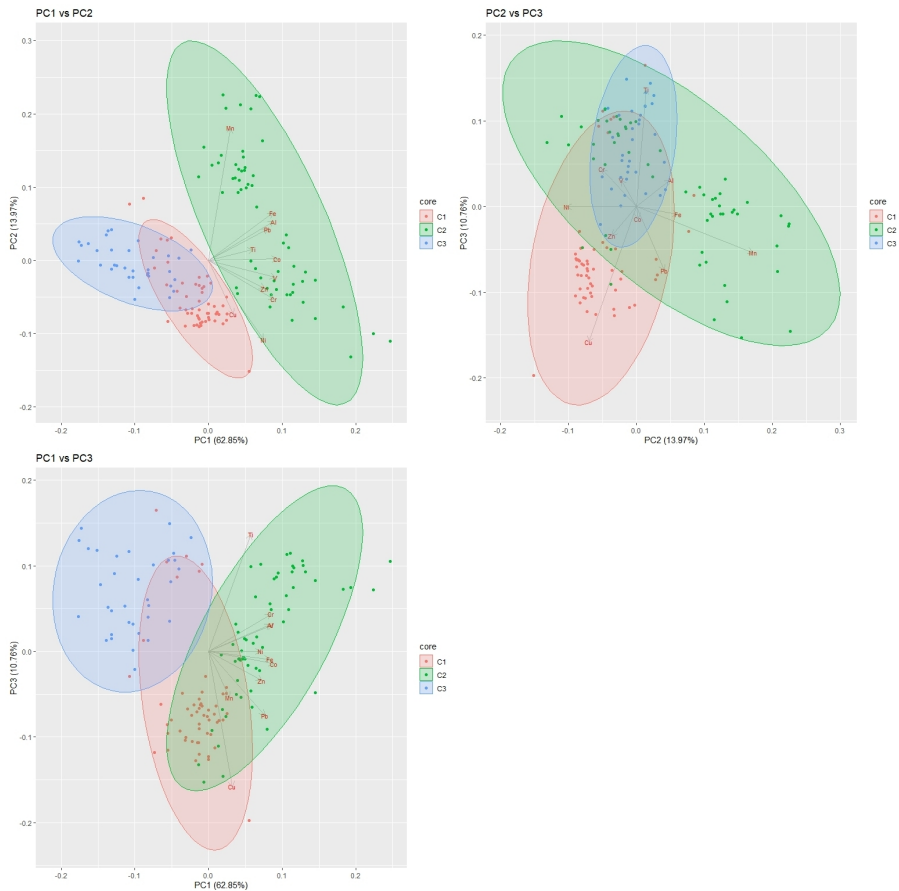


Fig. SM6: The graphs of the different principal components obtained through PCA implemented on the whole dataset of the 3 cores are reported, in order to observe the influence of the sampling site (C1,C2,C3).

Cluster Dendrogram C2

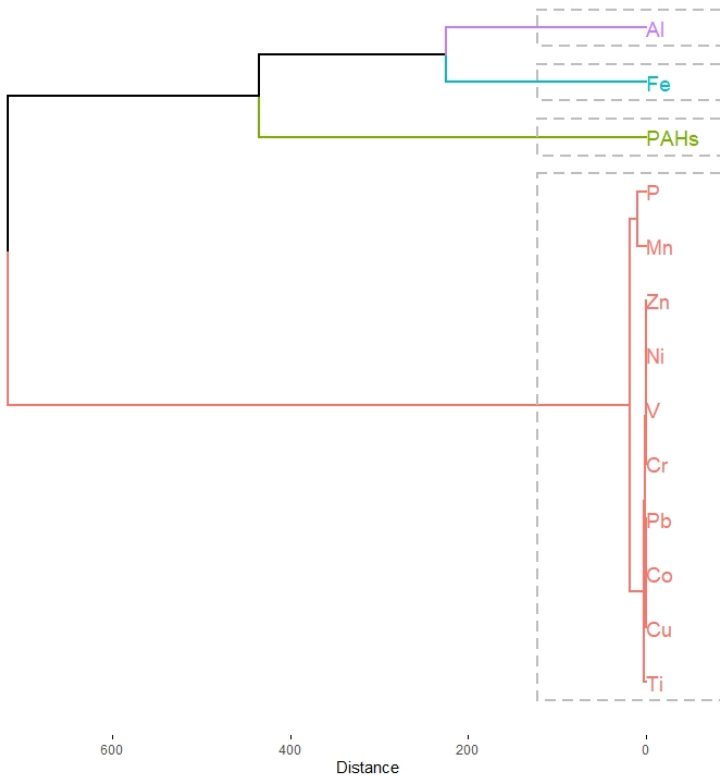


Fig. SM7: Hierarchical graph obtained with the cluster analysis for core C2 is shown. Al and Fe are grouped by the purple and blue boxes, PAHs by the green box, the other anthropogenic elements are grouped by the pink box, but Mn and P are indicated by a separate subgroup.

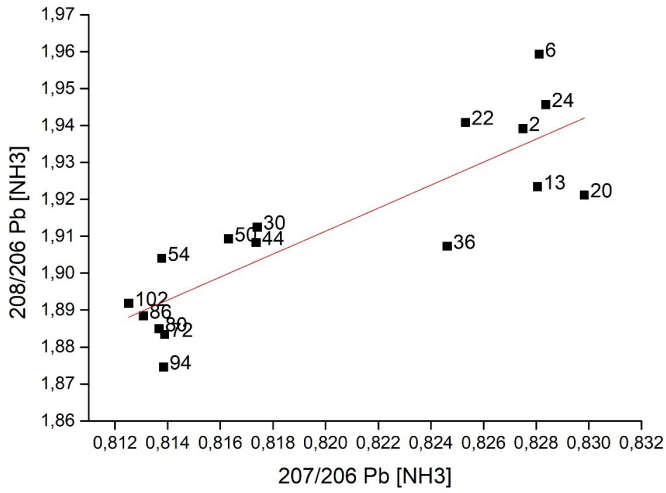


Fig. SM8: $^{208}\text{Pb}/^{206}\text{Pb}$ vs. $^{207}\text{Pb}/^{206}\text{Pb}$; the labels correspond to the sample number.